Chemical Technology, Prague, who kindly measured the M_n values, and Dr. O. Procházka from this institute for valuable discussions.

Registry No. (S)(I) (block copolymer), 105729-79-1.

References and Notes

(1) Benoît, H.; Froelich, D. In *Light Scattering from Polymer Solutions*; Huglin, M. B., Ed.; Academic: London, 1972; p 467.
(2) Eskin, V. Ye. *Rasseyaniye Sveta Rastvorami Polimerov*; Nauka: Moscow, 1973.
(3) Bushuk, W.; Benoît, H. *Can. J. Chem.* **1958**, *36*, 1616.
(4) Tuzar, Z.; Kratochvíl, P.; Straková, D. *Eur. Polym. J.* **1970**, *6*, 1113.
(5) Kotaka, T.; Donkai, N.; Min, T. I. *Bull. Inst. Chem. Res., Kyoto Univ.* **1974**, *52*, 332.
(6) Tanaka, T.; Omoto, M.; Donkai, N.; Inagaki, H. *J. Macromol. Sci., Phys.* **1980**, *B17*, 211.
(7) Stejskal, J.; Kratochvíl, P. *Polym. J.* **1982**, *14*, 603.
(8) Kuhn, R. *Makromol. Chem.* **1980**, *181*, 725.
(9) Dumelow, T.; Holding, S. R.; Maisey, L. J.; Dawkins, J. V. *Polymer* **1986**, *27*, 1170.
(10) Omoto, M.; Tanaka, T.; Kadokura, S.; Inagaki, H. *Polymer* **1979**, *20*, 129.
(11) Procházka, O.; Kratochvíl, P. *J. Polym. Sci., Polym. Phys. Ed.* **1983**, *22*, 501.
(12) Podešva, J. *Eur. Polym. J.* **1982**, *18*, 667.
(13) Ohnuma, H.; Kotaka, T.; Inagaki, H. *Polymer* **1969**, *10*, 501.
(14) Podešva, J.; Špaček, P.; Sikora, A.; Podol'skii, A. F. *J. Polym. Sci., Polym. Chem. Ed.* **1984**, *22*, 3343.
(15) Morton, M.; Fetters, L. J. *Rubber Chem. Technol.* **1975**, *48*, 359.
(16) Fetters, L. J. *J. Res. Natl. Bur. Stand., Sect. A* **1966**, *70*, 421.
(17) Millaud, B.; Strazielle, C. *Makromol. Chem.* **1979**, *180*, 441.
(18) Mrkvičková-Vaculová, L.; Kratochvíl, P. *Collect. Czech. Chem. Commun.* **1972**, *37*, 2015.
(19) Zimm, B. H. *J. Chem. Phys.* **1948**, *16*, 1099.
(20) van Wijk, R.; Staverman, A. J. *J. Polym. Sci., Polym. Phys. Chem.* **1966**, *4*, 1011.
(21) Tuzar, Z.; Kratochvíl, P. *Collect. Czech. Chem. Commun.* **1967**, *32*, 3358.
(22) Šimák, P.; Fahrbach, G. *Angew. Makromol. Chem.* **1970**, *12*, 73.
(23) Strazielle, C. In *Light Scattering from Polymer Solutions*; Huglin, M. B., Ed.; Academic: London, 1972; p 633.
(24) Kuhn, R. *Makromol. Chem.* **1984**, *185*, 1003.

Properties of Dimethylsiloxane Microphases in Phase-Separated Dimethylsiloxane Block Copolymers

Baoyu Wang and Sonja Krause*

Department of Chemistry, Rensselaer Polytechnic Institute, Troy, New York 12180.
Received January 12, 1987

ABSTRACT: Differential scanning calorimetry after fast, 200 K min^{-1}, and slow, 10 K min^{-1}, cooling rates was used to study the glass-transition temperature, T_g, and the crystallization and melting of dimethylsiloxane, DMS, microphases in styrene–dimethylsiloxane (S–DMS) block copolymers. The T_g's of amorphous DMS microphases in S–DMS diblock copolymers containing ≤28 wt % DMS were 6 K lower than the T_g = 145 K of slightly crystalline PDMS. This T_g lowering was apparently caused by thermal stress effects, as confirmed by calculations. Under the conditions of these experiments, DMS blocks with molecular weights ≤3800 did not crystallize, while those with molecular weights ≥15 400 were semicrystalline. The degree of crystallinity of semicrystalline DMS microphases which had been cooled from above the crystallization temperature at 10 K min^{-1} and then reheated at 10 K min^{-1} averaged 10% higher in samples containing ≥71 wt % DMS than in those containing ≤53 wt % DMS. These results are probably connected with the surface-to-volume ratios of the microphases. Single melting peaks were observed in samples that had been cooled at 10 K min^{-1}, while double melting peaks were observed in samples that had been cooled at 200 K min^{-1}.

Introduction

In a previous publication from this laboratory,[1] glass-transition data obtained by using differential scanning calorimetry (DSC) on dimethylsiloxane (DMS) microphases in some styrene–dimethylsiloxane (S–DMS) diblock copolymers were reported and discussed. Most of the DMS microphases made up of blocks with number-average molecular weights above 3600 were semicrystalline, but crystallization and melting data were not reported in that work because of problems with base lines in the crystallization and melting region obtained by using the DuPont 990 thermal analyzer. The DMS glass transitions of the amorphous DMS microphases were broadened relative to those of polydimethylsiloxane (PDMS), while the heat capacity change at the glass transition, ΔC_p, was comparable to that of PDMS. The T_g's of five fully amorphous DMS microphases were reported; one of these was 2 deg less than that of PDMS while the rest were 4–10 K higher than that of PDMS. The results were discussed qualitatively in terms of the thermal stress field that exists in these samples below the T_g of the styrene (S) microphases. This thermal stress field is caused by the unequal coefficients of thermal expansion of the two phases below the S microphase T_g. The rubbery DMS microphase has a larger thermal expansion coefficient than the glassy S microphase. When the rubbery DMS microphases are inclusions in the glassy PS matrix, these DMS inclusions are under a greater dilatational stress as the temperature decreases farther below the S microphases T_g. This dilatational stress is equivalent to a pressure decrease and thus leads to a decrease in the T_g of the DMS inclusions in the S microphase. The same argument holds for any rubbery inclusion in a glassy matrix. As an example, the thermal stress field in both phases in rubber-modified plastics such as high-impact polystyrene (PS) was studied by Paterno and Sternstein[2] who found that the dilatational stresses in the rubber particles should and do lead to a small decrease in T_g of these particles. Their work also indicates that an increase of the T_g of a rubbery microphase should be expected when this phase comprises the matrix instead of the inclusion. The calculations of the expected T_g increase are not straightforward and have not yet been attempted. The rubbery matrix should be able to sustain a stress field up to a few diameters away from the glassy inclusions. This leads to a small increase of the T_g. Earlier work by Beck et al.[3] only estimated the thermal stresses on rubbery inclusions in glassy matrices.

In the present work, the use of a much more accurate and precise DSC than that used in the previous work allowed us not only to obtain significant information on the

0024-9297/87/2220-2201$01.50/0

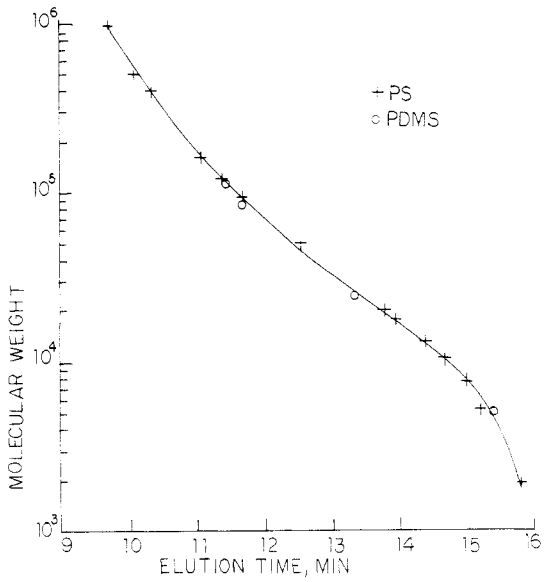

Figure 1. SEC calibration curve of PS and PDMS in chloroform.

crystallization and melting of a large number of DMS microphases but also to obtain accurate information on the effect of thermal stresses on the T_g of DMS microphases and to compare these with theoretical calculations.

Experimental Section

PDMS. Four samples of PDMS, ranging in molecular weight from 5000 to 1.1×10^5, $M_w/M_n \leq 1.21$[1,4] were used in this work.

Block Copolymers of S and DMS. Most of the S–DMS diblock copolymers have been described previously;[1] the rest of the diblock copolymers and all of the styrene–dimethylsiloxane–styrene triblock copolymers (S–DMS–S) were kindly supplied to us by J. Van Dusen of the Xerox Corporation.

Characterization. The number-average molecular weight (M_n), the weight-average molecular weight (M_w), and the molecular weight distribution of the block copolymer samples were determined by using size-exclusion chromatography (SEC) on a Knauer SEC apparatus from Utopia Instrument Co., Joliet, IL, equipped with a Knauer refractive index detector. Five Knauer lichrosphere columns with exclusion limits ranging from 5×10^3 to 4×10^6 daltons were used at 327 K with LC grade chloroform as solvent, 1% (w/v) polymer solutions, and a 1.00 mL min^{-1} flow rate through the columns. Figure 1 shows the calibration curve for a set of 15 PS standards, all with $M_w/M_n \leq 1.1$ and the four PDMS standards mentioned above. Since the calibration was the same for both homopolymers in this solvent (this was not the case in toluene which was used in the previous work), correct molecular weights were obtained without further calculation for all block copolymers whose refractive index did not match that of the solvent.

The compositions of the block copolymers were obtained by ^{1}H NMR by using a Varian XL-200 spectrometer. Five percent (w/v) solutions of polymer in a deuteriochloroform–carbon tetrachloride mixture were examined. The broad multiplet peak around δ 7.4 from the aromatic styrene ring and the triplet around δ from the DMS methyl protons were used for analysis.[1]

Differential Scanning Calorimetry (DSC). All measurements were performed on a Perkin-Elmer DSC-4 interfaced with an Ithaca Intersystems microcomputer using software from Laboratory Microsystems Inc., Troy, NY. Since all data on DMS microphases and PDMS were obtained below room temperature, liquid nitrogen was used as coolant and helium as the purge gas. Polymer samples weighing 15–20 mg were placed in flat aluminum DSC pans. Calibration of this instrument was described previously[5] except for the temperature calibration which was done by using 10 Fisher TherMetric standards whose melting points ranged from 177.5 to 423.5 K. Deviations of the measured melting points of the standards from those given by the supplier ranged up to 2 K. The PDMS and block copolymer samples were cooled at two different rates, 10 and 200 K min^{-1}, from above room temperature, and most of the data were collected during reheating at 10 K min^{-1}. A few crystallization data were collected during cooling. Glass-transition temperatures were obtained from heat capacity, C_p, vs. temperature, T, plots; the T_g was the temperature at which the experimental C_p vs. T curve crossed a point halfway between the extrapolated rubbery and glassy or semicrystalline base lines. The width of the glass transition, ΔT_g, was the difference between the temperatures at which the tangent to the C_p vs. T curve at T_g intersected the glassy or semicrystalline base line and the rubbery base line. The heat capacity change at the glass transition, ΔC_p, was the vertical distance between the extrapolated glassy or semicrystalline base line and the rubbery base line at T_g. These parameters have been shown graphically in Figure 1 of ref 1; the reasons for choosing the above definition of ΔT_g were discussed in ref 1. In the analysis of melting endotherms of DMS microphases, the high-temperature end of the melting peak was used as the melting point, T_m, of the microphase because of the generally large melting range of polymers. Melting points of nonpolymeric standards were taken as the temperature corresponding to the intersection between the extrapolated base line before the transition and the extrapolated leading edge of the melting transition peak. Heats of crystallization and fusion were calculated from the areas under the crystallization and melting peaks.

Results and Discussion

Block Copolymer Characterization. Table I shows the composition and molecular weight data obtained on the block copolymers used in this work. Diblock copolymer samples are designated DI-, and triblock copolymers are designated TR-. The designations of the 11 diblock copolymers, samples DI-1 through DI-5 and DI-9 through DI-14, that were studied previously[1] are also shown in Table I. Most of the samples had only a single peak in their SEC traces. Two samples, DI-3 and DI-8, however, showed a secondary peak and three samples, DI-1, DI-6, and DI-10, had a shoulder on the low molecular weight side of their SEC traces. This implies a small amount of homopolymer contamination in these samples as further shown by the fact that samples DI-6 and D-8 had the largest M_w/M_n ratios of any of the samples, 1.83 and 1.62, respectively. As usual with block copolymers, therefore, the samples with the largest M_w/M_n ratios had the broadest composition distributions. Chromatograms of some of the samples were obtained at different times to look for sample decomposition, but no changes were found. It should be noted that samples TR-4 and TR-5 were fractions of TR-3 and that samples TR-7 and TR-8 were fractions of TR-6. Previous SEC data on S-DMS diblock copolymers had been obtained in toluene solution[1] in which the homopolymers have different calibration curves. Data were nevertheless evaluated at that time as if the copolymers were PS. In the cases in which the block copolymers had DMS contents of about 50 wt %, the molecular weights estimated earlier in toluene solution are about 10% lower than the correct ones found in the present work. Samples DI-2 and DI-5, containing 68 and 71 wt % DMS, respectively, could not be measured in chloroform solution because their refractive indexes matched that of chloroform. It is also necessary to say that, because of the variation in refractive index of these block copolymers with composition, the M_w/M_n ratios of those samples that had an appreciable composition distribution are probably not correct. These samples include DI-1, DI-3, DI-6, DI-8, and DI-10. As will be seen below, however, errors of 10% or 20% in molecular weight have no effect on the conclusions drawn in this work.

Heat Capacity vs. Temperature for PDMS. Figure 2 shows C_p vs. T curves of a sample of high molecular weight PDMS obtained during heating at 10 K min^{-1} after cooling at 10 and 200 K min^{-1} from room temperature. After the slower cooling rate, the sample exhibited a glass

Table I
Molecular Characterization of the Block Copolymer Samples[a]

sample	wt % DMS	$\bar{M}_n \times 10^{-3}$	$\bar{M}_w \times 10^{-3}$	$\bar{M}_w/\bar{M}_n$	designation in ref 1
DI-1	14.0[b]	3.80 ± 0.3	4.90 ± 0.3	1.29 ± 0.04	I-24
DI-2	68.0[b]	4.40[b]	5.54[b]	1.26[b]	I-22
DI-3	41.0[b]	9.20 ± 0.1	10.5 ± 0.3	1.14 ± 0.02	I-15
DI-4	21.0[b]	7.90 ± 0.2	10.0 ± 0.2	1.26 ± 0.04	I-26
DI-5	71.0[b]	21.9[b]	25.0[b]	1.14[b]	I-29
DI-6	14.7 ± 0.3	6.80 ± 0.4	12.4 ± 0.4	1.83 ± 0.07	
DI-7	27.0 ± 0.6	7.40 ± 0.4	10.9 ± 0.5	1.47 ± 0.01	
DI-8	13.8 ± 0.6	17.1 ± 1.5	27.8 ± 1.6	1.62 ± 0.03	
DI-9	16.1[b]	19.2 ± 1.2	24.2 ± 1.5	1.05 ± 0.01	D-2
DI-10	12.1	22.6 ± 1.4	28.8 ± 1.5	1.27 ± 0.02	D-1
DI-11	53.0[b]	94.2 ± 1.9	111 ± 5	1.18 ± 0.03	R-15
DI-12	40.0[b]	182 ± 1.3	213 ± 1.6	1.16 ± 0.02	R-8
DI-13	34.0[b]	466	579	1.24	R-25
DI-14	42.0[b]	613 ± 14	745 ± 15	1.21 ± 0.01	R-26
DI-15	92.5 ± 0.3	48.2 ± 0.7	58.3 ± 4.0	1.11 ± 0.05	
DI-16	93.2 ± 0.3	79.0 ± 0.9	119 ± 3	1.51 ± 0.02	
TR-1	92.3 ± 0.2	34.2 ± 0.2	44.5 ± 4.0	1.30 ± 0.13	
TR-2	88.8 ± 0.3	49.8	74.6	1.50	
TR-3	92.8 ± 0.2	65.0 ± 5.0	88.0 ± 2.0	1.25 ± 0.04	
TR-4	87.2 ± 0.3	64.8 ± 1.1	80.7 ± 2.0	1.25 ± 0.01	
TR-5	94.3 ± 0.1	78.0 ± 0.9	95.2 ± 0.2	1.23 ± 0.03	
TR-6	93.0 ± 0.2	93.4 ± 8.0	142 ± 6	1.51 ± 0.02	
TR-7	91.2 ± 0.4	95.0	114 ± 10	1.30 ● 0.02	
TR-8	96.0 ± 0.2	150 ± 7.0	202 ± 10	1.33 ± 0.01	

[a] Errors shown are mean deviations. [b] Data from ref 1.

Table II
Glass Transition of DMS Microphases Collected on Heating at 10 K/min[a]

		after cooling at 10 K/min				after cooling at 200 K/min			
sample	$\bar{M}_n$(DMS) $\times 10^{-3}$	no. of runs	T_g, K	ΔT_g, K	ΔC_p, J/g K	no. of runs	T_g, K	ΔT_g, K	ΔC_p, J/g K
				Fully Amorphous Microphases					
DI-10	2.73	2	140 ± 1	15 ± 1	0.253 ± 0.004	1	141	10.5	0.232
DI-8	2.36	3	141 ± 1	15 ± 3	0.373 ± 0.054	2	141	14	0.493 ± 0.035
DI-6	1.00	3	143	16 ± 1	0.365 ± 0.049	3	143 ± 0.5	14.5 ± 1	0.318 ± 0.012
DI-9	3.09	3	141 ± 1	12 ± 2	0.171 ± 0.003	3	140 ± 1	15	0.249 ± 0.008
DI-4	1.66	3	130 ± 1	7 ± 3	0.212 ± 0.012	3	131 ± 0.5	12 ± 0.5	0.216 ± 0.012
DI-7	2.00	3	139 ± 2	10 ± 4	0.351 ± 0.040	3	139 ± 1.5	10.5 ± 2.5	0.310 ± 0.031
DI-3	3.77	2	147 ± 1	4 ± 1	0.351 ± 0.070	2	147.5 ± 1	7.5 ± 2	0.326 ± 0.011
DI-2	2.99	2	153.5 ± 0.5	7.5 ± 0.5	0.420 ± 0.022	2	150 ± 2	8 ± 1	0.426 ± 0.017
				Semicrystalline Microphases					
DI-13	158	3	147 ± 0.5	4.5 ± 0.5	0.167 ± 0.008	3	146 ± 0.5	4.5 ± 0.5	0.195 ± 0.009
DI-12	72.8	3	147 ± 1	8 ± 1	0.108 ± 0.007				
DI-14	257	2	149.5 ± 1	10.5 ± 0.5	0.098 ± 0.007	2	150	12.5 ± 0.5	0.134 ± 0.009
DI-11	49.9	3	150 ± 2	10 ± 4	0.073 ± 0.012	3	148 ± 1	9 ± 2	0.160 ± 0.079
DI-5	15.4	3	154 ± 2	16 ± 3	0.100 ± 0.005	3	147 ± 2	3 ± 1	0.450 ± 0.050
TR-4	56.7	3	150 ± 2	15 ± 3	0.065 ± 0.008	3	147 ± 1	3 ± 0.5	0.360 ± 0.070
TR-2	44.2	3	153 ± 1	12 ± 1	0.110 ± 0.009	3	146 ± 2	3 ± 0.5	0.120 ± 0.010
TR-7	86.6	3	152 ± 1	17 ± 2	0.084 ± 0.008	3	146 ± 1.5	7.5 ± 4	0.130 ± 0.030
TR-1	31.6	3	153 ± 0.5	11 ± 3	0.078 ± 0.020	3	146 ± 1	3 ± 1.5	0.420 ± 0.030
DI-15	44.6	3	149 ± 1	17 ± 2	0.091 ± 0.010	3	147	3 ± 1	0.371 ± 0.005
TR-3	60.3	3	150 ± 1	13 ± 3	0.110 ± 0.013	3	147.5 ± 1	3	0.421 ± 0.008
TR-6	86.9	3	149 ± 1	12 ± 2	0.077 ± 0.007	3	146 ± 1.5	3 ± 0.5	0.400 ± 0.020
DI-16	79.9	3	149 ± 1	13 ± 3	0.074 ± 0.006	3	147 ± 0.5	3 ± 0.5	0.410 ± 0.007
TR-5	73.6	3	152 ± 1	16 ± 3	0.073 ± 0.008	3	149 ± 2	7 ± 4	0.349 ± 0.026
TR-8	144	3	149 ± 1	12 ± 1	0.098 ± 0.008	3	148 ± 2	6.5 ± 4	0.181 ± 0.050
PDMS-2	24.3	2	150 ± 1	13 ± 1	0.074 ± 0.005	2	145	4 ± 0.5	0.431 ± 0.003
PDMS-3	84.1	2	150 ± 0.5	12 ± 1	0.147 ± 0.009	2	145 ± 0.5	3 ± 0.5	0.434 ± 0.005
PDMS-4	111	2	151 ± 1	14 ± 1	0.101 ± 0.006	2	146 ± 1	3.5 ± 1	0.395 ± 0.005

[a] Errors shown are mean deviations.

transition (not easily seen on Figure 2) and a doublet melting transition, while, after cooling at 200 K min^{-1}, the sample showed an appreciable glass transition and a large crystallization exotherm as well as a doublet melting transition. Doublet melting peaks have been observed by a number of other workers[6-9] in samples of PDMS. Clarson et al.[9] reported that very low molecular weight PDMS, $M_n \leq 2460$, had only a single melting peak. A secondary melting peak emerged as a shoulder at a higher temperature when the PDMS M_n increased to 2900. The area under the second melting peak increased with molecular weight, the peaks became more separated from each other, and, finally, the higher temperature melting peak became dominant at $M_n = 2.55 \times 10^4$. The doublet melting peak has been variously attributed to reorganization of small, imperfect crystallites during heating[7,8] or to different crystal forms of PDMS,[9] although only one crystal structure has been reported for this polymer.[10]

Experimental data on the PDMS glass transitions are shown in Table II together with similar data on the DMS

Table III
Melting Points and Heats of Melting and Crystallization of DMS Microphases[a]

	after cooling at 10 K/min and reheating at 10 K/min			after cooling at 200 K/min and reheating at 10 K/min			
sample	no. of runs	T_m, K	ΔH_m, J/g	no. of runs	T_m, K	ΔH_m, J/g	ΔH_c, J/g
DI-13	3	235 ± 1	20.6 ± 0.7	3	236 ± 1	19.8 ± 1.1	
DI-12	2	235	15.5 ± 0.5	2	236 ± 1	14.0 ± 0.5	5.61 ± 0.16
DI-14	3	234 ± 1	14.7 ± 0.8	3	234 ± 0.5	14.1 ± 0.5	
DI-11	3	234 ± 1	18.7 ± 0.5	3	236 ± 1	19.1 ± 1.5	2.40 ± 0.41
DI-5	3	237 ± 0.5	25.3 ± 0.8	3	238 ± 1	25.1 ± 0.9	18.7 ± 1.9
TR-4	3	237 ± 1	23.9 ± 0.7	3	236	22.1 ± 1.3	14.7 ± 0.3
TR-2	3	234 ± 1.5	21.3 ± 1.2	3	235 ± 1	22.5 ± 0.5	6.1 ± 2.4
TR-7	3	236 ± 1	21.8 ± 1.2	3	236 ± 0.5	22.6 ± 0.2	6.4 ± 1.6
TR-1	3	236 ± 1	24.8 ± 0.3	3	236 ± 0.5	22.9 ± 0.3	19.1 ± 0.4
DI-15	2	238	22.6 ± 0.3	3	237 ± 1	22.9 ± 0.6	19.6 ± 0.9
TR-3	3	237 ± 1.5	24.0 ± 0.3	3	239 ± 2	25.2 ± 0.4	16.2 ± 0.1
TR-6	3	237 ± 1	23.6 ± 0.2	3	237 ± 1.5	22.1 ± 1.1	18.2 ± 0.5
DI-16	3	237 ± 1	24.4 ± 0.3	3	236 ± 1	23.5 ± 0.8	16.4 ± 1.9
TR-5	3	236 ± 1.5	23.5 ± 0.4	3	237 ± 2	22.4 ± 0.5	6.3 ± 1.4
TR-8	3	235 ± 1	21.7 ± 1.2	3	237 ± 0.5	24.9 ± 0.4	5.7 ± 3.4
PDMS-2	2	240	30.6 ± 0.4	2	238.5 ± 0.5	30.7 ± 0.1	23.2 ± 0.5
PDMS-3	2	239 ± 1	35.2 ± 0.2	2	240	36.8 ± 0.8	28.3 ± 0.3
PDMS-4	2	240 ± 1	36.0 ± 0.3	2	240 ± 1	37.1 ± 0.4	28.7 ± 0.4

[a] Errors shown are mean deviations.

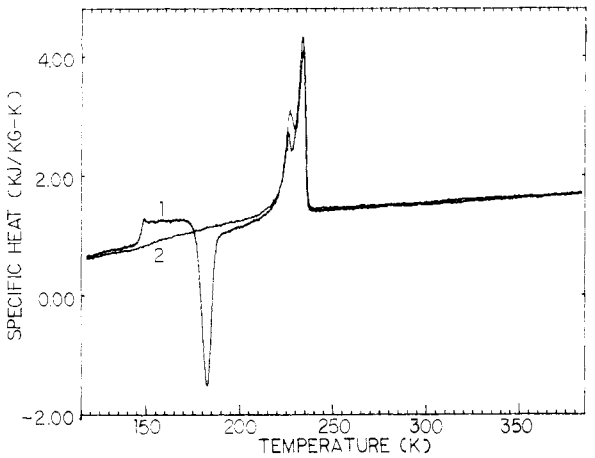

Figure 2. Specific heat vs. temperature of PDMS, M_n = 1.11 × 10^5, after cooling at (1) 200 and (2) 10 K min^{-1}.

microphases in the block copolymers. The PDMS samples cooled from room temperature at 10 K min^{-1} had T_g's of 150 K, with ΔT_g's of 13 K. The PDMS samples cooled at 200 K min^{-1} had T_g's of 145 K, with ΔT_g's ≤ 4 K. The difference in the T_g values after the different cooling rates is connected with the difference in percent crystallinity of the samples at the glass transition after the different cooling rates. After 200 K min^{-1} cooling, the samples were about 14% crystalline at T_g, while after 10 K min^{-1} cooling, they were 50–59% crystalline at T_g (see Tables III and IV). All of the PDMS crystallites form inclusions in an amorphous PDMS matrix. They can thus exert thermal stresses on the matrix, densifying it slightly as mentioned above for rubbery matrices surrounding glassy inclusions. Probably, the T_g's of the samples cooled at 200 K min^{-1} are very close to the T_g of fully amorphous PDMS. We would thus like to propose 145 K as the T_g of high molecular weight PDMS, in contrast to the values of 148–150 K proposed in a previous paper from this laboratory[1] and by many others.[8,9,11-16] These previous values were obtained on PDMS samples and networks of unspecified crystallinity. The fact that increasing crystallinity increases the T_g of PDMS has been noticed by others[17] but has apparently not affected the estimates of the T_g of amorphous PDMS in the literature.

Table V shows the C_p values below the glass transition and above the melting transition of a high molecular weight

Table IV
Degree of Crystallinity of Semicrystalline Microphases[a]

	α_F, %		α_I, %
sample	after cooling at 10 K min^{-1}	after cooling at 200 K min^{-1}	after cooling at 200 K min^{-1}
DI-13	33.7 ± 1.1	32.4 ± 1.7	32.4 ± 1.7
DI-12	25.3 ± 0.9	22.9 ± 0.9	13.7 ± 0.9
DI-14	24.0 ± 1.3	22.9 ± 0.9	22.9 ± 0.9
DI-11	30.6 ± 0.9	31.3 ± 2.4	27.4 ± 2.5
DI-5	41.4 ± 1.3	41.0 ± 1.5	10.4 ± 3.4
TR-4	39.0 ± 1.1	36.1 ± 2.2	12.1 ± 2.2
TR-2	35.8 ± 2.0	36.8 ± 0.9	26.8 ± 4.0
TR-7	35.7 ± 2.0	37.0 ± 0.2	26.5 ± 2.7
TR-1	40.5 ± 0.4	37.4 ± 0.4	6.2 ± 0.8
DI-15	37.0 ± 0.4	34.4 ± 0.9	5.3 ± 1.8
TR-3	39.2 ± 0.4	41.2 ± 0.7	14.8 ± 0.7
TR-6	38.5 ± 0.2	36.1 ± 1.8	6.4 ± 2.0
DI-1	39.9 ± 0.4	38.3 ± 1.3	11.5 ± 3.2
TR-5	38.3 ± 0.7	36.6 ± 0.9	26.3 ± 2.4
TR-8	35.5 ± 0.2	40.7 ± 0.7	31.5 ± 5.6
PDMS-2	50.0 ± 0.7	50.2 ± 0.2	12.3 ± 0.9
PDMS-3	57.5 ± 0.2	60.1 ± 1.3	13.9 ± 1.4
PDMS-4	58.8 ± 0.4	60.6 ± 0.7	13.7 ± 0.9

[a] α_F is the final percent crystallinity just before the melting transition, and α_I is the initial percent crystallinity at the glass transition; the error limits are the mean deviations from the average values.

Table V
Specific Heat of PDMS-4 at Various Temperatures, Collected on Heating at 10 K/min

T, K	C_p,[a] J/g K	C_p,[b] J/g K	T, K	C_p,[a] J/g K	C_p,[b] J/g K
120	0.660	0.639	305	1.538	1.575
125	0.717	0.682	310	1.551	1.592
130	0.754	0.717	315	1.558	1.615
135	0.783	0.765	320	1.573	1.625
140	0.824	0.799	325	1.570	1.627
245	1.438	1.485	330	1.594	1.631
250	1.439	1.487	335	1.608	1.644
255	1.446	1.487	340	1.601	1.640
260	1.462	1.492	345	1.612	1.656
265	1.476	1.522	350	1.625	1.658
270	1.467	1.508	355	1.656	1.681
275	1.488	1.519	360	1.643	1.668
280	1.513	1.535	365	1.664	1.689
285	1.508	1.535	370	1.683	1.694
290	1.516	1.551	375	1.690	1.693
295	1.526	1.550	380	1.685	1.704
300	1.532	1.561	385	1.720	1.722

[a] After cooling at 200 K min^{-1}. [b] After cooling at 10 K min^{-1}.

PDMS sample after both cooling rates. Each set of numbers is the average of two runs. Values obtained after the two cooling rates generally agree within ≈3%. When the values shown in Table IV are compared either with those of Turdakin et al.[12] or Lebedev et al.[16] and recommended by Gaur et al.,[18] the deviation is within ≈2% for the data collected after 10 K min^{-1} cooling and within ≈5% for that collected after 200 K min^{-1} cooling. We do not report values of C_p between the glass transition and T_m because these depend on the degree of crystallinity of the samples.

Crystallization and Melting of DMS Microphases. Under all the conditions used in this work, DMS microphases with $M_n \leq 3800$ did not crystallize, while those with $M_n \geq 1.54 \times 10^4$ always became semicrystalline. Such a change in crystallizability with molecular weight is common in block copolymers. Godovskii et al.[19] for example, found that DMS microphase crystallization did not occur in samples of acrylate–dimethylsiloxane block copolymers having DMS block $M_n \leq 3700$ even after annealing for 10 h at the optimum crystallization temperature. Studies on styrene–ethylene oxide multiblock copolymers[20] showed that the ethylene oxide blocks did not crystallize at block $M_n = 404$ and crystallized only slightly at block $M_n = 900$, slightly more at block $M_n = 1960$, and finally, to an appreciable extent at block $M_n = 5650$. The crystallization of the DMS and ethylene oxide microphases just cited, as well as the DMS microphases in our S–DMS block copolymers, occurs in the presence of another glassy microphase. The glassy microphases thus exert a constraint on the crystallization of the DMS or ethylene oxide microphases in the sense that a portion of the crystallizable segments in the block copolymers, those near the interfaces with the glassy microphases, are constrained from undergoing the conformational changes necessary for crystallization. Therefore, crystallizability of the microphases should decrease as the surface area to volume ratio, A/V, of the microphases increases. In block copolymers, there is a variation of A/V with morphology. In addition, for all samples morphologies, the A/V increases as block molecular weight decreases. It is thus logical that there should be a lower limit to the block molecular weight at which crystallization can occur in block copolymers.

DSC traces collected during cooling at 10 K min^{-1} on some of the homopolymers and crystallizable block copolymers exhibited one crystallization exotherm each. Microphases with $M_n \geq 3.2 \times 10^4$ in samples with high, >90 wt %, DMS content and homopolymers had crystallization exotherms with peaks at 201 to 205 K, while two DMS microphases, one with $M_n = 5.0 \times 10^4$ and 53 wt % DMS in the copolymer and the other with $M_n = 1.54 \times 10^4$ and 71 wt % DMS, had crystallization exotherms with peaks at 185 to 186 K. The A/V ratios of the last two DMS microphases are expected to be greater than those in the very high DMS content block copolymers; therefore, the observed changes in crystallization temperature during cooling are probably also connected with the A/V ratio. It should be more difficult to crystallize microphases with a higher A/V ratio, as discussed above, so the greater supercooling of these samples before they crystallize seems reasonable.

Figure 3 shows some representative DSC curves taken on reheating some of the semicrystalline block copolymers after different cooling rates. In contrast to PDMS, most of the DMS microphases had only a single melting peak after cooling at 10 K min^{-1} as shown by curve 1 on Figure 3. Only samples DI-5 and DI-15 showed evidence of a double melting peak after this cooling rate. Just as in PDMS, no crystallization occurred in any of the DMS

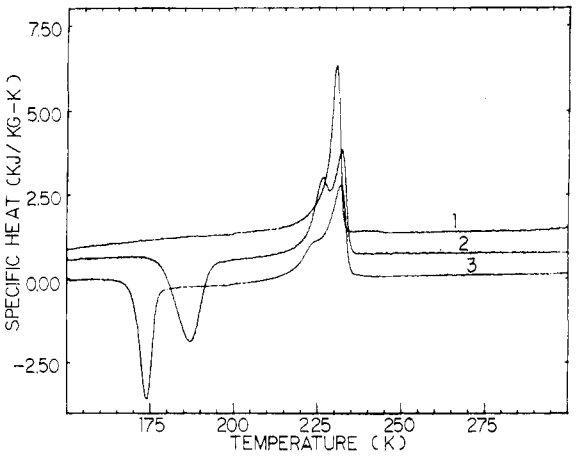

Figure 3. Specific heat vs. temperature of (1) TR-7 after 10 K min^{-1} cooling, (2) TR-1 after 200 K min^{-1} cooling, and (3) DI-16 after 200 K min^{-1} cooling. The ordinate is for curve 1; the other curves are shifted downward progressively by 0.6 J g^{-1} K^{-1}.

microphases during reheating at 10 K min^{-1} after the same cooling rate. After 200 K min^{-1} cooling, however, both crystallization and melting peaks were observed in all the semicrystalline samples except for samples DI-13 and DI-14 which had only a melting peak. Most of the melting peaks were doublets except for samples DI-12, DI-13, and DI-14, which had single melting peaks after 200 K min^{-1} cooling. Thus, most of the DMS microphases had single melting peaks and no crystallization peaks on reheating after 10 K min^{-1} cooling, but doublet melting peaks and crystallization peaks on reheating after 200 K min^{-1} cooling. Therefore, with the few exceptions cited above, the crystallites formed during cooling either had a different crystal structure or different crystallite size or perfection than those formed during reheating.

Table III shows the crystallization and melting data obtained after both cooling rates on DMS microphases and on PDMS samples. The T_m's of all the DMS microphases were between 234 and 238 K, all slightly lower than the 239–240 K found for PDMS. After 10 K min^{-1} cooling, the DMS microphases containing >53 wt % DMS had T_m from 234 to 235 K, while those containing >70 wt % DMS had T_m from 237 to 238 K. After 200 K min^{-1} cooling, on the other hand, the variation in T_m appeared to be random. Since the enthalpy of crystallization, ΔH_c, was always smaller than the enthalpy of fusion, ΔH_m, (see Table III) some crystallization always occurred during cooling, even at 200 K min^{-1}.

Degree of Crystallinity of DMS Microphases. The enthalpy of fusion of PDMS, $\Delta H°_m = 61.19$ J g^{-1},[16] was used to calculate the degree of crystallinity of each DMS microphase after the two cooling rates. In Table IV, α_F is the final percent crystallinity achieved by each microphase after all crystallization was complete, and α_I is the initial degree of crystallinity achieved by each microphase during cooling at 200 K min^{-1}:

$$\alpha_I = 100(\Delta H_m - \Delta H_c)/\Delta H°_m \quad (1)$$

Table IV shows that α_F was about the same for all the DMS microphases and PDMS samples after both cooling rates. Figure 4 shows these values vs. the wt % DMS in the block copolymers. Figure 4 emphasizes the fact that the four block copolymers containing ≤53 wt % DMS had α_F values lower than those of the many block copolymers that contained ≥71 wt % DMS. Table IV shows that even these latter block copolymers had α_F values at least 10% lower than those of PDMS. This variation in final percent

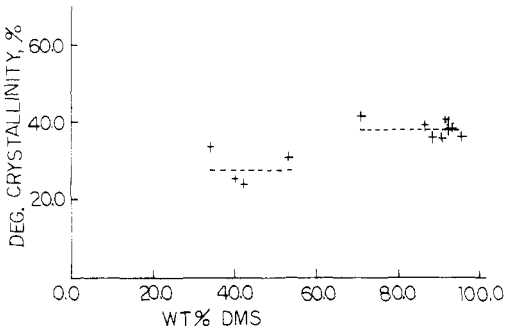

Figure 4. Final degree of crystallinity, α_F, vs. wt % DMS in the block copolymers. The dotted lines indicate the average degrees of crystallinity for the two groups of microphases.

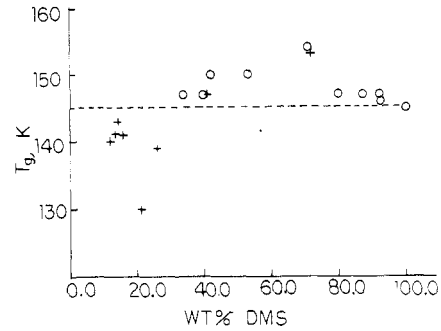

Figure 5. Glass-transition temperature vs. wt % DMS in the block copolymers. The crosses are for fully amorphous DMS microphases and the circles are for semicrystalline DMS microphases with ≤15% crystallinity. The dotted line indicates the T_g of almost amorphous PDMS, 145 K.

crystallinity is probably connected with block copolymer morphology. In any of the block copolymers, no matter how high the wt % DMS, the DMS must crystallize under the constraints of the attached S microphases. It is therefore reasonable that all the block copolymers should have lower values of α_F than the homopolymers. Furthermore, DMS segments that exist in lamellar, cylindrical, or spherical DMS microphases (≤53 wt % DMS) are under more constraints than those that exist in a DMS matrix microphase (≥71 wt % DMS).

The Glass Transition. Table II shows the glass transition data on all DMS microphases and homopolymers after the two cooling rates. The first eight samples in the Table were completely amorphous after both cooling rates; these samples had DMS microphases with $M_n \leq 3800$. All other samples, including the homopolymers, were semicrystalline. In general, the T_g's of the semicrystalline DMS microphases were lower after 200 K min^{-1} cooling than they were after 10 K min^{-1} cooling, except for samples DI-13 and DI-14, which had the same percent crystallinity after both cooling rates. All other DMS microphases, as shown in Table IV, had a lower percent crystallinity at the glass transition, α_I, after 200 K min^{-1} cooling than after 10 K min^{-1} cooling. As in the case of PDMS homopolymers, phases with higher crystallinity have higher T_g's. Even the DMS microphases with degrees of crystallinity as low as those of PDMS after 200 K min^{-1} cooling had T_g's averaging 2 deg higher than those of these PDMS samples. The DMS microphases have thermal stresses arising from the presence of both the crystallites and the S microphases, both causing an increase in T_g for these microphases, which are all, by the way, in block copolymers having ≥40 wt % DMS. The greater the percent crystallinity at the glass transition, the larger the observed value of ΔT_g for both the DMS microphases and the PDMS samples. The DMS repeat units near the attached crystallites are under thermal stress and should therefore undergo the glass transition at a slightly higher temperature than the DMS repeat units farther from the crystallites. This explanation is consistent with the increase of both ΔT_g and T_g with increasing crystallinity. The ΔC_p's of most of the microphases and homopolymers, even the fully amorphous microphases, were less than the value of 0.50 J g^{-1} obtained by Godovskii et al.[17] for liquid nitrogen quenched, presumably 100% amorphous PDMS. In the case of the semicrystalline phases, this ΔC_p decrease may be attributed to the fact that the crystalline DMS segments are not undergoing the glass transition. In the case of the fully amorphous DMS microphases, some of the DMS segments are often mixed into the styrene, S, microphases and undergo the glass transition with the S segments. This mixing has been discussed previously[1] and will be further discussed later.[21,22]

There is essentially no difference between the T_g's obtained on the fully amorphous DMS microphases after the two different cooling rates. Most of the T_g's, however, are lower than those of the almost amorphous PDMS samples. Figure 5 shows the T_g's of these fully amorphous DMS microphases vs. the wt % DMS in the block copolymers. Samples with wt % DMS ≤ 27% have T_g's that average 139 ± 3 K, while the two amorphous DMS microphases in samples with 41 and 72 wt % DMS have an average T_g of 150 K. Thus, the samples containing such low percentages of DMS that the DMS microphases are almost certainly inclusions in an S matrix have T_g's that are, on the average, depressed 6 K below that of almost amorphous PDMS. This depression of the T_g is almost certainly caused by dilatational thermal stresses and will be discussed and calculated below. The T_g's of the microphases in the samples with higher DMS content are slightly elevated above that of almost amorphous PDMS as are those of the DMS microphases which had very low percent crystallinity at the glass transition; these are also shown in Figure 5. All these slightly crystalline DMS microphases were in block copolymers containing ≥34 wt % DMS. It is a moot point whether the sample with 34 wt % DMS consisted of cylindrical inclusions of DMS in an S microphase or whether this sample had a lamellar morphology. At any rate, for most of the amorphous or almost amorphous DMS microphases with T_g's above that of almost amorphous PDMS, the slight increase of T_g was that expected for a DMS matrix around an S inclusion.

The magnitude of the thermal stresses and thus the lowering of the T_g of the DMS inclusions in the S matrix can be estimated by using the equations developed by Paterno and Sternstein[2] for isolated spherical rubbery inclusions in a glassy matrix. As a first approximation, the change of T_g with pressure was assumed constant

$$\delta T_g/\delta P = D \tag{2}$$

where P is pressure and D is a constant that is not known for PDMS, so that we used the average of the values[23] for polyisoprene, polybutadiene, and polyisobutylene, $\Delta T_g/\delta P = 0.23$ K MPa^{-1}, for our calculations. The thermal stresses, σ_i, in the DMS inclusions were estimated by using[2]

$$\sigma_i = [-2E_2(\alpha_1 - \alpha_2)\Delta T(1 - f)]/K \tag{3}$$

where E_2 is the Young's modulus of the glassy matrix, α_1 and α_2 are the thermal expansion coefficients of the rubber and glass, respectively, ΔT is the difference between the T_g of the matrix and the temperature of interest, f is the volume fraction of the rubbery inclusions, and K is

$$K = 2f(1 - 2\nu_2)(1 + \alpha_1\Delta T) + (1 + \nu_2)(1 + \alpha_1\Delta T) + (2E_2/E_1)(1 - 2\nu_1)(1 - f)(1 + \alpha_2\Delta T) \tag{4}$$

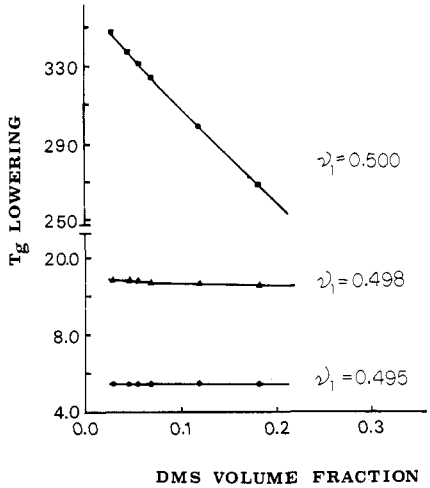

Figure 6. Calculated T_g lowering due to thermal stresses of DMS spherical inclusions in an S matrix vs. volume fraction DMS in the block copolymer when E_1 = 2.10 MPa.

where E_1 is the Young's modulus of the rubber and ν_1 and ν_2 are the Poisson's ratio of the rubbery inclusions and the glassy matrix, respectively. The magnitude of the stress estimated from eq 4 is in only one dimension. The lowering of T_g, however, is proportional to the three-dimensional dilatational stress which is equal to the first invariant in the rubber, three times the calculated value of σ_i in this case.

The values of material properties used for the glassy matrix were those of bulk PS: $E_2 = 2.8 \times 10^3$ MPa, $\nu_2 = 0.35$, and $\alpha_2 = 0.8 \times 10^{-4}$.[24] The thermal expansion coefficient of PDMS, $\alpha_1 = 9.1 \times 10^{-4}$,[25] was used for the DMS inclusions. Since values of Young's modulus or Poisson ratio were not found for PDMS, the coefficient of isothermal compressibility of high molecular weight PDMS, 1.238×10^{-3} cm^3 J^{-1},[26] was converted to the bulk modulus which, together with the shear modulus, can be used to calculate both the Young's modulus and the Poisson ratio. The reported values of the shear modulus of cross-linked PDMS range from 0.669 to 2.07 MPa.[27] This range of shear moduli gave values of ν_1 equal to almost exactly 0.5 and a range of E_1 values of 2.10–6.21 MPa. The weight fractions of DMS in the block copolymers were converted to volume fractions by using 1.05 g cm^{-3} [24] for the density of PS, and 1.00 g cm^{-3} [25] for the density of PDMS. A value of −200 K, near the DMS T_g's, was used for ΔT.

Figure 6 shows the calculated δT_g of the DMS inclusions in an S matrix by using E_1 = 2.10 MPa and values of ν_1 equal to 0.5 and two other values near 0.5. The Poisson ratio of 0.500 gives impossible values of δT_g, below 0 K. A Poisson ratio of 0.495, however, gives a δT_g close to the 6 K actually observed (see Figure 5). Figure 6 shows that very small changes, <1%, in the Poisson ratio have a large effect on the calculated T_g of the rubbery inclusions. The effect of changing E_1 at constant ν_1 is not as dramatic. For example, if ν_1 is held constant at 0.495, then $\delta T_g \approx 12$ K when E_1 is increased to 6.1 MPa. A decrease of E_1 to 0.63 MPa, on the other hand, gives a $\delta T_g \approx 2$ K. Thus, the T_g of the rubbery DMS inclusions is not extremely sensitive to changes in their Young's modulus.

Because of the uncertainty in the material parameters of PDMS, and also because the microphases in block copolymers are not isolated, we can only demonstrate that reasonable values of the material parameters of PDMS lead to the observed values of the T_g's. Furthermore, when the rubbery inclusions are not isolated, the stress field in the matrix will be different, and thus the stress field in the inclusions will also be affected.

Conclusions

1. The correct T_g of amorphous PDMS after 200 K min^{-1} and 10 K min^{-1} cooling rates is 145 ± 0.5 K. When the PDMS is appreciably crystalline, its T_g increases to about 150 K, probably due to the thermal stresses induced in the amorphous DMS matrix surrounding the DMS crystallites.

2. Fully amorphous DMS microphases in S–DMS block copolymers containing ≤28 wt % DMS had T_g's that were 6 ± 3 K lower than the proposed value for amorphous PDMS. This T_g lowering was apparently caused by thermal stress effects, as confirmed by calculations. Fully amorphous and slightly crystalline DMS microphases in block copolymers containing ≥34 wt % DMS had T_g's very close to those of appreciably crystalline PDMS. This T_g increase was also attributed to thermal stress effects.

3. DMS blocks with molecular weights ≤3800 did not crystallize under the conditions used in this work, while those with molecular weights ≥15 400 became partly crystalline.

4. The degree of crystallinity of semicrystalline DMS microphases which had been cooled from room temperature at 10 K min^{-1} and then reheated at 10 K min^{-1} averaged 10% higher in samples containing ≥71 wt % DMS than in those containing ≤53 wt% DMS. These results were connected with the different surface-to-volume ratios of the microphases.

5. Single melting peaks were observed in DMS microphases which had been cooled at 10 K min^{-1}, while doublet melting peaks were observed after 200 K min^{-1} cooling. It is not known whether the doublet melting peaks are due to crystallites of different size and perfection or to different crystal forms of PDMS.

Acknowledgment. We thank C. I. Chung, Materials Engineering, for the use of the Perkin-Elmer DSC-4, and we thank J. Van Dusen of the Xerox Corporation for some of the S–DMS block copolymers. We also thank the National Science Foundation, Polymers Program, for partial support of this work through Grant DMR81-06107. Special thanks are given to S. S. Sternstein, Materials Engineering, for valuable discussions of the thermal stress effect.

References and Notes

(1) Krause, S.; Iskandar, M.; Iqbal, M. *Macromolecules* **1982**, *15*, 105–111.
(2) Paterno, J. J. Ph.D. Thesis, Rensselaer Polytechnic Institute, Troy, NY, 1970. Sternstein, S. S., private communication.
(3) Beck, R. H.; Gratch, S.; Newman, S.; Rusch, K. C. *Polym. Lett.* **1968**, *6*, 707–709.
(4) Iqbal, M., unpublished work from this laboratory.
(5) Granger, A. T.; Wang, B.; Krause, S.; Fetters, L. J. *Adv. Chem. Ser.* **1986**, 127–138.
(6) Slonimskii, G. L.; Levin, V. Y. *Vysokomol. Soedin. Ser. A* **1966**, *8*, 1936–1941; *Polym. Sci. USSR (Engl. Transl.)* **1966**, *8*, 2139–2144.
(7) Yagfarov, M. S.; Ionkin, V. S. *Vysokomol. Soedin., Ser. A* **1968**, *10*, 1613–1617; *Polym. Sci. USSR (Engl. Transl.)* **1986**, *10*, 1867–1873.
(8) Lee, C. L.; Johannson, O. K.; Flaningam, O. L. *Polym. Prepr. (Am. Chem. Soc., Div. Polym. Chem.)* **1969**, *10*, 1311–1318.
(9) Clarson, S. J.; Dodgson, K.; Semlyen, J. A. *Polymer* **1985**, *26*, 930–934.
(10) Damaschun, G. *Kolloid-Z.* **1962**, *180*, 65–67.
(11) Cowie, J. M. G.; McEwen, I. J. *Polymer* **1973**, *14*, 423–426.
(12) Turdakin, V. A.; Tarasov, V. V.; Mal'tsev, A. K. *Zh. Fiz. Khim.* **1976**, *50*, 1980–1984; *Russ. J. Phys. Chem. (Engl. Transl.)* **1976**, *50*, 1192–1195.
(13) Adachi, H.; Adachi, K.; Ishida, Y.; Kotaka, T. *J. Polym. Sci., Polym. Phys. Ed.* **1979**, *17*, 851–857.
(14) Weir, C. E.; Leser, W. H.; Wood, L. A. *J. Res. Natl. Bureau Stand.* **1950**, *44*, 367–372.
(15) Polmanteer, K. E.; Hunter, M. J. *J. Appl. Polym. Sci.* **1959**, *1*, 3–10.

(16) Lebedev, B. V.; Mukhina, N. N.; Kulagina, T. G. *Vysokomol. Soedin., Ser. A.* **1978**, *20*, 1297–1303; *Polym. Sci. USSR (Engl. Transl.)* **1979**, *20*, 1458–1466.
(17) Godovskii, Y. K.; Levin, V. Y.; Slonimskii, G. L.; Zhdanov, A. A.; Andrianov, K. A. *Vysokomol. Soedin., Ser. A* **1969**, *11*, 2444–2451; *Polym. Sci. USSR (Engl. Transl.)* **1969**, *11*, 2778–2786.
(18) Gaur, W.; Lau, C.; Wunderlich, B. *J. Phys. Chem. Ref. Data* **1983**, *12*, 91–108.
(19) Godovskii, Y. K.; Dubovik, I. I.; Papkov, V. S.; Valetskii, P. M.; Dolgoplosk, S. B.; Slonimskii, G. L.; Vinogradova, S. V.; Korshak, V. V. *Dokl. Akad. Nauk SSSR* **1977**, *232*, 105–107; *Dokl. Phys. Chem. (Engl. Transl.)* **1977**, *232*, 4–6.
(20) Shimura, Y.; Hatakeyama, T. *J. Polym. Sci., Polym. Phys. Ed.* **1975**, *13*, 653–662.
(21) Wang, B. Ph.D. Thesis, Rensselaer Polytechnic Institute, Troy, NY, 1987.
(22) Wang, B.; Krause, S., manuscript in preparation.
(23) Anderson, J. E.; Davis, D. D.; Slichter, W. P. *Macromolecules* **1969**, *2*, 166–169.
(24) Brandrup, J., Immergut, E. H., Eds. *Polymer Handbook*, 2nd ed.; Wiley: New York, 1980.
(25) Shih, H.; Flory, P. J. *Macromolecules* **1972**, *5*, 758–761.
(26) Weissler, A. *J. Am. Chem. Soc.* **1949**, *71*, 93–95.
(27) Valles, E. M.; Rost, E. J.; Macosko, G. W. *Rubber Chem. Technol.* **1984**, *57*, 55–62.

Dynamic Viscoelastic Properties of ABS Polymers in the Molten State. 5. Effect of Grafting Degree

Yuji Aoki

Yokkaichi Research and Development Department, Mitsubishi Monsanto Chemical Co., Ltd., Toho-cho, Yokkaichi, Mie 510, Japan. *Received January 23, 1987*

ABSTRACT: Dynamic viscoelastic and steady-flow properties of molten ABS polymers with different grafting degree were measured by using a concentric cylinder-type rheometer. It was found that the viscoelastic functions, in terms of storage shear modulus G' and loss shear modulus G'' as a function of angular frequency ω and shear stress τ as a function of shear rate $\dot{\gamma}$, depend strongly on grafting degree in the long-time region associated with particle–particle interactions. As the grafting degree increases, the viscoelastic functions first decrease and then increase. The minima in the functions occurred at the grafting degree of about 0.45 for ABS polymers having rubber particle size of 170 nm. When the grafting degree is below or above 0.45, second-plateau regions in G' and yield stresses in the flow curves were observed in the long-time region. Observation of the state of dispersion of rubber particles by transmission electron microscope revealed that the rubber particles of samples having the minima in the viscoelastic functions are finely dispersed but that those of the other samples exhibiting second plateaus or yield stresses form an agglomerated or a three-dimensional network structure of rubber particles. Relationship between grafting degree and colloidal stability of rubber particles is also discussed.

Introduction

Recently, many kinds of rubber-modified thermoplastic polymers have been developed and used in industrial fields. By blending of rubber component to rigid polymers, impact strength of the polymer is improved, while the other properties, for example, modulus and processability, are generally deteriorated. Therefore, it is very important for development of rubber-modified polymers to find how to improve the impact strength without deterioration of the other properties.

ABS (acrylonitrile–butadiene–styrene) polymers are one of the most typical rubber-modified polymers commercialized at about 3 decades ago. Manufacturing of ABS polymers first was made by blending of AS (acrylonitrile–styrene) copolymer and rubber. Nowadays, ABS polymers of graft type are made by copolymerizing styrene and acrylonitrile monomers in the presence of rubber. During the polymerization some of the AS copolymers become grafted to the rubber. These grafted AS copolymers act as a dispersing agent. Physical properties of ABS polymers are influenced by not only the rubber content, rubber particle size, and molecular weight of the matrix AS copolymer, but also the quantity, composition, and molecular weight of the grafted AS copolymer on the surface of rubber particles.

We have made model ABS polymers by emulsion polymerization and studied dynamic viscoelastic properties of the polymers in the molten state for several years.[1-6] We found that there are two kinds of ABS polymers, each having a different dynamic behavior.[1,2] One kind has the second-plateau region. In other words, it exhibits the pseudoequilibrium modulus (G_e) that storage shear modulus G' does not depend on frequency at a low frequency, as was previously found by Zosel[7] and Moroni and Casale;[8] the other does not have the second-plateau region and its G' decreases with a lowering of frequency. The former was found in the systems in which rubber particles agglomerate in the matrix phase (or form three-dimensional network structure), while the latter was found in finely dispersed systems without agglomerated structure. It was also found that the viscoelastic properties of ABS polymers are influenced by acrylonitrile content (AN%) in grafted AS copolymers[3] and by rubber particle size.[4,6] When the difference in AN% between grafted and matrix AS copolymers was small, the rubber particles were dispersed finely without agglomeration, and no G_e was found. The mismatching of AN% caused the agglomeration of particles and led to the observation of G_e in these ABS systems. We also reported that the long-time relaxation spectra of ABS polymers having good dispersion of particles are remarkably affected by the rubber particle size.[4,6]

Huguet and Paxton made some model ABS polymers in which the amount of graft is varied for several particle sizes of rubber and found that the melt viscosities of these polymers first decrease and then increase as the grafting degree increases.[9] Their measurement was made by a capillary rheometer and then was limited at high shear rate. Rheological properties of ABS polymers show anomalous behavior in the long-time region.[1-10] Therefore, it is of interest to study the relationship between the grafting degree and the rheological properties in the long-time region.

In this paper, we made model ABS polymers in which only the amount of grafted AS copolymers is varied, and

0024-9297/87/2220-2208$01.50/0